HHS Public Access

Author manuscript

J Immunol. Author manuscript; available in PMC 2019 June 15.

Published in final edited form as:

J Immunol. 2018 June 15; 200(12): 3942–3949. doi:10.4049/jimmunol.1800259.

Slit2 modulates the inflammatory phenotype of orbit-infiltrating fibrocytes in Graves' disease

Roshini Fernando, **Ana Beatriz Diniz Grisolia**, **Yan Lu**, **Stephen Atkins**, and **Terry J. Smith**

Department of Ophthalmology and Visual Sciences, Kellogg Eye Center, and Division of Metabolism, Endocrinology, and Diabetes, Department of Internal Medicine, University of Michigan Medical School, Ann Arbor, MI 48105

Abstract

Human $CD34^+$ fibrocytes, circulating monocyte lineage progenitor cells, have recently been implicated in thyroid-associated ophthalmopathy (TAO), the ocular manifestation of Graves' disease (GD). Fibrocytes express constitutive MHC-2 and surprisingly thyroglobulin (Tg) and functional thyrotropin receptor (TSHR). Underlying expression of these thyroid proteins is the autoimmune regulator protein (AIRE). Fibrocytes respond robustly to TSH and thyroid-stimulating immunoglobulins (TSI) by generating extremely high levels of inflammatory cytokines such as IL-6. In TAO, they appear to infiltrate the orbit where they transition to $CD34^+$ orbital fibroblasts ($CD34^+$ OF). There, they coexist with $CD34^-$ OF as a mixed fibroblast population (GD-OF). In contrast to fibrocytes, GD-OF express vanishingly low levels of MHC-2, Tg, TSHR, and AIRE. Further, the amplitude of IL-6 induction by TSH in GD-OF is substantially lower. The molecular basis for this divergence between fibrocytes and $CD34^+$ OF remains uncertain. Here we report that Slit2, an axon guidance glycoprotein, is constitutively expressed by the $CD34^-$ OF subset of GD-OF. Culture medium conditioned by incubating with GD-OF and $CD34^-$ OF (CM) substantially reduces levels of MHC-2, Tg, TSHR, and AIRE in fibrocytes. Expression can be restored by specifically depleting CM of Slit2. The effects of $CD34^-$ OF CM are mimicked by rhSlit2. TSH induces Slit2 levels in GD-OF by enhancing both Slit2 gene transcription and mRNA stability. These findings suggest that Slit2 represents a TSH-inducible factor within the TAO orbit that can modulate the inflammatory phenotype of $CD34^+$ OF and therefore may determine the activity and severity of the disease.

Introduction

Fibrocytes derived from the monocyte lineage appear to play critical roles in tissue remodeling and wound healing (1–3). They display a $CD45^+CD34^+CXCR4^+$Col I^+ phenotype, constitutively express high levels of major histocompatibility complex Class II (MHC-2), and several co-activation molecules through which they engage in complex bidirectional interactions with T cells (4, 5). They produce a diverse array of

Person to whom reprint requests should be addressed: Terry J. Smith, M.D., Department of Ophthalmology and Visual Sciences, Kellogg Eye Center, University of Michigan Medical School, 1000 Wall Street, Ann Arbor, MI, 48105 Phone: (734) 764-0435 Fax: (734) 232-8021 terrysmi@med.umich.edu.

Permanent address of Dr. Lu: Department of Ophthalmology, Jinling Hospital, School of Medicine, Nanjing University, Nanjing 210002, Jiangsu Province, China.

immunologically impactful molecules including cytokines (2, 6). Fibrocyte differentiation depends on T cells (4). Unexpectedly, fibrocytes express several autoantigens (7) including "thyroid-specific" proteins such as thyroglobulin (Tg), thyrotropin receptor (TSHR), sodium-iodide symporter, and thyroperoxidase (7–10). Expression of these thyroid proteins in fibrocytes is dependent on autoimmune regulator protein (AIRE) (10).

Fibrocytes have recently been implicated in the pathogenesis of several autoimmune diseases, including rheumatoid arthritis (11), type I diabetes mellitus (12), and Graves' disease (GD) (13, 14). In GD, orbital connective tissues surrounding the eye become infiltrated with T and B cells, mast cells and fibrocytes which appear to participate in the development of thyroid-associated ophthalmopathy (TAO). TAO remains a vexing, disfiguring, and potentially blinding condition without effective and safe medical therapies (15). A critical question remaining to be answered is why some patients with GD develop severe eye disease while others do not manifest any ocular abnormalities. By virtue of their display of functional TSHR, fibrocytes can produce proinflammatory cytokines in response to both TSH and the pathogenic, TSHR-activating immunoglobulins (TSI) that drive hyperthyroidism of GD (13, 16, 17). Once in the TAO orbit, fibrocytes transition to $CD34^+$ orbital fibroblasts ($CD34^+$OF). There they coexist with residential $CD34^-$ OF in a mixed fibroblast population (GD-OF). Yet GD-OF fail to express the high Tg and TSHR levels found in fibrocytes cultured from the circulation (8, 10). Vanishingly little is currently known about the factors generated within the human orbit that determine the behavior of infiltrating cells recruited from the bone marrow. We proffer that $CD34^-$ OF exert a modulating influence(s) on $CD34^+$ OF, resulting in the dramatically lower expression levels of MHC-2, thyroid proteins, and AIRE, a phenomenon that has remained unexplained. Fibrocytes may represent a critical link between the autoimmunity occurring within the thyroid and orbit in GD yet the factor(s) regulating expression of thyroid-related proteins by these cells once they infiltrate the orbit remains unidentified.

Slit2, an axonal guidance/repellent glycoprotein, constrains neuron migration and enforces midline integrity in the developing brain (18, 19). Three different mammalian orthologs of Slit have been identified (18). Members of the Slit family negatively influence leukocyte chemotaxis (20, 21) and mediate chemo-repulsion of diabetogenic T cells (22). The Slit2 pathway has been implicated in the regulation of angiogenesis and appears to alter the clinical behavior of human cancers (23). Its expression correlates with tumor outcome (24). Slit2 acts through its cognate receptor, ROBO1, a surface transmembrane glycoprotein displayed on target cells (25). Recent evidence suggests that the Slit2/ROBO1 pathway plays a regulatory role in fibrocyte differentiation into lung fibroblasts and thus helps determine tissue remodeling in fibrotic lesions (26). Healthy lung tissues secrete Slit2 and attenuate the differentiation of fibrocytes while Slit2 expression is diminished in tissue surrounding lung fibrosis (26).

Here we report that Slit2 appears to underlie the substantial differences in MHC-2, AIRE and thyroid-related gene expression found in peripheral blood mononuclear cell (PBMC)-derived fibrocytes compared with GD-OF. $CD34^-$ OF constitutively express and release Slit2, levels of which are increased by TSH. Conditioned medium (CM) generated from mixed GD-OF and pure $CD34^-$ OF reduces levels of MHC-2, Tg, TSHR, and AIRE in

fibrocytes while neutralizing Slit2 restores their expression. Recombinant human Slit2 (rhSlit2) mimics the inhibitory effects of $CD34^-$ OF. The expression of these proteins and the induction by TSH of IL-6 were found to be attenuated through mechanisms involving AIRE gene transcription. These findings suggest that Slit2, expressed by $CD34^-$ OF in the TAO orbit, can modulate the inflammatory phenotype of $CD34^+$ OF and thus could determine disease behavior and outcome.

Materials and Methods

Materials

Fetal bovine serum (FBS, cat.# 16000-044), Dulbecco's modified Eagle medium (DMEM, cat.# 11965) containing 4.5 g/mL D-Glucose and L-Glutamine, penicillin-streptomycin mixture (cat.# 15140), protein G magnetic beads (cat.# 10004D) and Dynabead magnet (cat.# 12321D) were supplied by Life Technologies (Grand Island, NY). rhSlit2 (cat.# SRP3155) was from Sigma-Aldrich (St. Louis, MO). Human Slit2 sandwich ELISA (cat.# LS-F12612) was supplied by LifeSpan BioSciences Inc.(Seattle, WA). 5,6-dichlorobenzimidazole (DRB) came from Cayman (Ann arbor, MI, cat.# 10010302). bovine TSH (bTSH) was from Calbiochem (La Jolla, CA, cat.# 609385). M22, an activating anti-TSHR monoclonal antibody (27) was from Kronus (Star, ID, cat.# M22-5c/00-690). Anti-mouse CD34 IgG 1- FITC (cat.# 555822), anti-human MHC-2 (HLA-DR)-PE (cat.# 555812), anti-mouse IgG1 isotype control-PE (cat.# 555749) and Fixation and Permeabilization solution (cat.# 554722) were from BD Biosciences, San Diego, CA. Accutase (cat,# SCR005) was from Millipore, Billerica, MA. Human $CD34^+$ nucleofection kit (cat.# VPA-1003) was supplied by Lonza, Allendale, NJ. Rabbit anti-Slit2 (EPR2771) Ab (cat.# ab134166), rabbit anti-Hsp47 (EPR4217) Ab (cat.# ab109117), anti- AIRE Ab (cat.# ab65040) and anti-thyroglobulin Ab (cat.# 156008) came from Abcam, Cambridge, MA. Anti-rabbit Alexa Fluor 488 secondary Ab was from Life technologies. Anti-TSHR Ab (3B12) was from Santa Cruz, Dallas, TX (cat.# sc-53542). Isotype-matched rabbit IgG (cat.# 011-000-003) was from Jackson ImmunoResearch, West Grove, PA. Anti-human Slit2 ChiP Ab (cat.# PA5-31133) and Pierce Agarose ChiP kit (cat.# 26156) were from Thermo Fisher, Rockford, IL. Anti-ROBO1 Ab (cat.#MAB71181) was from R & D systems (Minneapolis, MN). siRNA targeting Slit2 (cat.# L-019853-00-10) and its control (cat.# D-001810–10-5) were from Dharmacon (Lafayette, CO). Slit2 ChIP assay (cat.# 334001) was from QIAGEN (Germantown, MD).

GD-OF and fibrocyte isolation and cultivation

Peripheral blood and surgical waste were obtained as approved by the Institutional Review Board of the University of Michigan Health System from an academic endocrine and ophthalmology practice. All subjects gave written and verbal informed consent. GD-OFs were cultivated from deep orbital connective tissues removed during surgical decompression for TAO. A total of 10 GD-OF strains, each from a different donor, were used in these studies. Cultivation of GD-OF has been published previously (28) and were used between passages 2–11, an interval when cell phenotypes remained stable.

Fibrocytes were cultured from PBMCs, provided by the American Red Cross or from patients with GD or healthy individuals. PBMCs from a total of 30 different donors were used in these studies. They were isolated by Ficoll Histopaque density gradient centrifugation and cultivated as originally described (1). Six-well plates were inoculated with 7×10^6 PBMCs and covered with DMEM supplemented with 10% FBS. After 10–14 days, adherent monolayers (<5% of the starting population) were rinsed and removed by mechanical scrapping without or with accutase. Cell viability was >90% by trypan blue exclusion and >90% were fibrocytes as routinely assessed using a BD LSR flow cytometer (BD Biosciences) (29).

Flow cytometry and cell sorting

Viable cells were gated and data analyzed by comparing signals to isotype controls using the FCS Expression software program (De Novo software, Ontario, CA). Cytometric cell sorting of GD-OF followed staining for 30 min at 4°C with fluorescein isothiocynate-conjugated anti-mouse CD34 mAb or its isotype. Washed cells were sorted under sterile conditions with a FACSAria III (BD Biosciences). GD-OF (mixed, pure $CD34^+$, and pure $CD34^-$ subsets) were re-cultured for 48 h prior to their use in experiments.

RNA preparation and real-time PCR

Cellular RNA was extracted from monolayers with the Aurum ™ Total RNA Mini Kit (cat.# 732-6820, Bio-RAD, Hercules, CA). RNA (2 μg) was reverse-transcribed and real-time PCR performed using an Applied Biosystems instrument with QuantiTect SybrGreen PCR kit (cat.# 204143, Qiagen, Frederick, MD). Primer sequences were: GAPDH; forward, 5’-TTGCCATCAATGACCCCTTCA-3’, reverse, 5’-CGCCCCACT-TGATTTTGGA-3’, IL-6; forward, 5’-TGAGAAAGGAGACATGTAACAAGAGT-3’, reverse, 5’-TTGTTCCTCACTACTCTCAAATCTGT-3’; Tg; forward, 5’-GAGCCCTACCTCTTCTGGCA-3’, reverse, 5’-GAGGTCCTCATTCCTCAGCC-3’; AIRE; forward, 5’-CCCTACTGTGTGTGGGTCCT-3’, reverse, 5’-ACGTCTCCTGAGCAGGATCT-3’. Primers for hSlit2 (cat.# PPH05968A), MHC-2 (cat.# PPH05538B), and TSHR (cat.# PPH02344C) were from QIAGEN. PCR values were generated against a standard curve and normalized to respective GAPDH signals.

Cell transfections

Gene promoter fragment activities were assessed by transfecting fibrocytes and GD-OF using the U-023 program of Nucleofector™ II instrument (LONZA, Allendale, NJ.) with the Amaxa™ human CD34 cell nucleofection kit (cat.# VPA-1003; LONZA). Gene promoter fragment sequences were: Slit2, −2414 to +556 nt; AIRE, −1200 to +1 nt (Dr. Part Peterson (Tartu); Tg, −181bp to +16bp (Professor Samuel Refetoff, Univ Chicago); ICA69, −1012 to +19 nt (A.L. Notkins, NIH). Slit2 knockdown was conducted by transfecting GD-OF with specific a targeting siRNA using methods we have described previously (10).

Depletion of Slit2 from GD-OF and $CD34^-$ OF CM

CM were generated by incubating parental GD-OF, pure $CD34^-$ OF, and $CD34^+$ OF (control) for 48 h. These were then immune-adsorbed with rabbit anti-Slit2 Ab (Cat#

134166, Epitomic/Abcam) while anti-HSP47 and isotype-matched IgG were controls. Briefly, protein G magnetic beads were coated with Abs for 2 h, washed using a Dynamagnet × 3 and incubated with 500 μl CM overnight at 4C. Media were added to fibrocyte cultures and incubated for 7 d. Monolayers were lysed, RNA extracted, and cDNAs subjected to RT- PCR.

Slit2 chromatin immuneprecipitation (ChIP) assay

ChIP assays were performed with a Pierce Agarose ChIP kit following manufacturer's protocol.

Statistics

Statistical significance was determined with the two-tailed Student's *t* test. $p<0.05$ was considered statistically significant.

Results

Levels of constitutive AIRE, MHC-2, Tg, and TSHR expression and TSH-inducible IL-6 diverge in fibrocytes and GD-OF

GD-OF comprise $CD34^+$Col I^+CXCR4^+ OF and thus fulfill the criteria for fibrocytes (29). They are admixed with $CD34^-$Col I^-CXCR4^- OF (13). The latter represent native residential OF. Despite the well-represented presence of $CD34^+$ OF in GD-OF (approximately 50%), levels of AIRE, MHC-2, Tg, and TSHR are dramatically lower in GD-OF than in fibrocytes (Fig. 1A–1D; AIRE mRNA, 766 ± 4 vs 22 ± 5 ($p<0.001$); MHC-2 mRNA, 323 ± 12 vs 2 ± 0.3 ($p<0.001$); Tg mRNA, 28 ± 1 vs 2 ± 0.3 ($p<0.001$); TSHR mRNA, 28 ± 2 vs 3 ± 0.6 ($p<0.001$). Similarly, the induction by bTSH (5 mIU/mL) of IL-6 mRNA and protein was greater in fibrocytes compared to GO-OF (Fig. S1A and S1B, both $p<0.001$).

The potential for $CD34^-$ OF to express a factor(s) that modulates gene expression in $CD34^+$ OF was explored by sorting GD-OF into pure $CD34^+$ and $CD34^-$ subsets (Fig. 2A). Levels of the 4 protein-encoding transcripts are considerably higher in $CD34^+$ OF than in $CD34^-$ OF (AIRE; 14-fold ($p<0.001$), MHC-2; 6-fold ($p<0.001$), Tg; 3-fold ($p<0.01$), and TSHR; 12-fold ($p<0.01$) or parental GD-OF (AIRE; 3-fold ($p<0.001$), MHC-2; 2.5-fold ($p<0.01$), Tg; 2-fold ($p<0.001$) and TSHR; 8-fold ($p<0.01$). Further, the induction of IL-6 mRNA by bTSH is greater in $CD34^+$ OF compared to $CD34^-$ OF 13-fold, ($p<0.001$) and parental GD-OF (7-fold, $p<0.001$) (Fig. S1C). Thus $CD34^-$ OF appear to generate a factor(s) attenuating protein expression in $CD34^+$ OF and modulate the induction by TSH of IL-6.

The inhibitory factor appears to be soluble and is released from $CD34^-$ OF. CM generated from parental GD-OF, pure $CD34^+$ OF and $CD34^-$ OF were used to cover fibrocyte monolayers for 5 d. Levels of AIRE, MHC-2, Tg, and TSHR mRNAs were substantially higher in fibrocytes incubated with CM from $CD34^+$ OF compared to CM from either $CD34^-$ OF (AIRE; 13-fold ($p<0.001$), MHC-2; 4-fold ($p<0.001$), Tg; 16-fold ($p<0.01$) and TSHR; 5-fold ($p<0.01$) or parental GD-OF (AIRE; 13-fold($p<0.001$), MHC-2; 3-fold ($p<0.001$), Tg; 7-fold ($p<0.01$), and TSHR; 2-fold ($p<0.01$) (Fig. 2B).

A recent report indicated that Slit2 can block fibrocyte differentiation (26). Thus, determining whether Slit2 might play some role in altering gene expression repertoire in GD-OF and fibrocytes appeared potentially informative. CM from parental GD-OF and pure $CD34^-$ OF subsets was Slit2-depleted by immune-adsorption and used to cover fibrocytes. Slit2 depletion of these CM restored expression of AIRE (3-fold, $p<0.01$), MHC-2 (1.5-fold, $p<0.01$), Tg (2-fold, $p<0.01$), and TSHR (2.5-fold, $p<0.05$) compared to isotype-treated CM (Fig. 3A). Knocking down Slit2 expression in GD-OF with siRNA specifically targeting Slit2 substantially enhanced levels all four mRNAs (Fig. 3B, AIRE (3-fold, $p<0.01$), MHC-2 13-fold, $p<0.001$), Tg (2-fold, $p<0.01$), TSHR (6-fold, $p<0.001$). These results imply that Slit2 generated by $CD34^-$ OF can modulate gene expression in fibrocytes and GD-OF.

GD-OF express basal and TSH-inducible Slit2

Several strains of GD-OF were examined for basal and TSH-inducible Slit2 mRNA. As Fig. 4A demonstrates, Slit2 transcripts are essentially undetectable in untreated fibrocytes, levels that were not appreciably induced by bTSH. In contrast, Slit2 mRNA is constitutively expressed in GD-OF while bTSH (5 mIU/mL) induces Slit2 mRNA 75-fold ($p<0.01$) and protein in a time-dependent manner, peaking at 12 h (Fig.4B, 30-fold ($p<0.001$). Slit2 expression by GD-OF localizes strongly to the $CD34^-$ OF subset (Fig. S2A). Conversely, levels of its cognate receptor, ROBO1, are higher in fibrocytes and $CD34^+$ OF compared to $CD34^-$ OF (Fig. S2B).

To determine whether the cell-type selective Slit2 expression pattern resulted from divergent gene promoter activity, a 2970 bp fragment of the human Slit2 promoter (−2414 nt to +556 nt) was cloned, fused to PGL3, and transfected into GD-OF and fibrocytes. Its activity was appreciably higher in GD-OF (180 ± 5.1) compared with fibrocytes (0.6 ± 0.1)($p<0.001$, Fig. 4C). Further, the promoter activity was considerably higher in pure $CD34^-$ OF compared with $CD34^+$ OF (Fig.S2C, $p<0.01$). The upregulation of Slit2 expression by bTSH appears to be mediated by enhanced gene transcription. RNA Pol II occupancy was increased by bTSH in GD-OF after 2 h (21.63 ± 0.02 vs untreated control, 0.08 ± 0.01)($p<0.001$, 22-fold difference, Fig. 4D). In addition, Slit2 mRNA is stabilized by bTSH (Fig. 4E, 31-fold difference, $p<0.01$) at 12 h. Thus the induction of Slit2 by bTSH is mediated through both transcriptional and post-transcriptional mechanisms

rhSlit2 down-regulates specific protein expression in fibrocytes

When added to the medium of differentiated fibrocytes, rhSlit2 (50ng/ml) fails to alter CD34 display (Fig. S3) while reducing AIRE (52%, $p<0.01$), MHC-2 (73%, $p<0.001$), Tg (66%, $p<0.01$), and TSHR (69%, $p<0.001$) protein in fibrocytes (Fig. 5A) compared to untreated controls. rhSlit2 also attenuates the induction by bTSH at 6 h of AIRE (78%, $p<0.01$), Tg (51%, $p<0.01$), and TSHR (76%, $p<0.01$) (Fig.5B). The down-regulation of TSHR carries functional consequences. bTSH-dependent induction of IL-6 mRNA and protein are also reduced by Slit2 (mRNA, 65%, protein 37%, both $p<0.01$ versus control) and M22 (mRNA 69%, protein 57%, both $p<0.01$) (Fig. S1D, S1E).

The mechanism through which rhSlit2 attenuates AIRE and Tg expression in fibrocytes was examined by transfecting cells with respective gene promoter/reporter constructs into control

and rhSlit2-treated cells (Fig.S4A). rhSlit2 dramatically down-regulated the activities of both promoter fragments (80.9% ($p<0.01$) and 67.5% ($p<0.05$), respectively). Slit2 failed to influence the activity of ICA69, suggesting specificity of these effects. In contrast, changes in AIRE mRNA and Tg mRNA stabilities do not account for the effects of Slit2 on levels of these proteins (Fig. S4B).

Discussion

Slit/ROBO pathways play what appear to be diverse regulatory roles in brain development, several other healthy tissues, and various forms of cancer (30). In the central nervous system, Slit2 governs the path in which axons from retinal ganglion cells must traverse and thereby restricts the tissues that are targeted within the embryonic diencephalon (31). These actions on neuronal guidance are mediated through Ca^{2+} dependent mechanisms (32). In glioma, Slit2 inactivates Cdc-42, a Rho GTPase, and in so doing inhibits cell migration (33). The actions of Slit2 are complex as a consequence of multiple intersections between Slit2/ROBO1 and other pathways. This is exemplified by the relationship between miR-218 and its host gene, *Slit2*, in various forms of cancer (34). In some tissues, Slit2 has been found to antagonize VEGF (35).

The involvement of Slit2 in extra-neural processes is now being recognized. Its impact on immunity suggests a generally inhibitory influence that may modulate the inflammatory response. Slit2 and its orthologues appear to regulate the immune system and host defense. In monocytes, through its interactions with ROBO1, Slit2 inhibits monocyte chemotaxis and the stabilization of monocyte adhesion tethered to endothelium (36). Slit2 is upregulated during allergen sensitization and inhibits the migration of hapten-induced Langerhans cells *in vitro* and *in vivo* and in so doing, attenuates hypersensitivity responses (37). The Slit2/ROBO1 pathway mediates stromal cell-derived factor-1-dependent repulsion of pathogenic T cells in pancreatic islet vascular endothelium (22).

Slit2 has been identified as a factor governing the participation of fibrocytes in lung fibrosis (26). Those earlier findings demonstrated that Slit2 can inhibit fibrocyte differentiation from monocytes. Further, Slit2 is expressed by fibroblasts surrounding fibrocytes *in vivo* at sites of tissue injury and dampens differentiation. In contrast, fibrotic tissues appear to express lower levels of the protein which may have been inadequate in holding fibrocyte differentiation in check. In contrast, the current studies examine the impact of Slit2 on fibrocytes following their differentiation by assessing the expression of specific genes relevant to TAO. The questions posed by the current line of inquiry concerns the activities of fibrocytes that have infiltrated the diseased orbit. We find that Slit2, encoded by a TSH-inducible gene, is expressed selectively by $CD34^{-}$OF and is responsible, at least in part for the divergence between the relatively high levels of AIRE, Tg, TSHR, and MHC-2 found in fibrocytes when compared to those in GD-OF (Fig. 1). The induction of Slit2 by TSH is mediated at both transcriptional and post-transcriptional levels and may underlie the well-recognized activation of TAO in the clinical setting of poorly controlled thyroid hormone levels (38). The effects of rhSlit2 on Tg and TSHR expression on the other hand are mediated through changes in gene promoter activity. Thus, Slit2 can regulate the expression of genes directly implicated in the pathogenesis of TAO by influencing the two principal

orbital self-antigen candidates in GD and by lowering MHC-2 levels in fibrocytes. It is therefore possible that the actions of Slit2 may impose a modulatory effect on immune reactivity occurring in ocular GD. The impact of Slit2 on fibrocyte/T cell interactions is currently being investigated in our laboratory.

TAO is typically self-limited and dominated initially by inflammation associated with fat and muscle expansion (38). Mechanisms underlying the transition from active to stable disease have yet to be identified. Further, the question of why some patients with GD fail to develop TAO while others manifest sight-threatening disease remains uncertain. The unique attributes of fibrocytes and their presence in the TAO orbit strongly suggest their involvement in disease pathogenesis (10, 13). But whether they determine disease duration, amplitude, and severity has remained unexplored. We propose that an orbital factor(s), perhaps Slit2, might modulate the fibrocyte phenotype locally as they transition into $CD34^+$ OF and could influence the behavior of these cells *in situ*. Fibrocytes activated by TSH and TSI generate remarkably high levels of several cytokines (39). The current findings demonstrate that Slit2 can markedly diminish the capacity of fibrocytes to generate proinflammatory cytokines such as IL-6 in response to TSH and M22. Thus the tissue context surrounding fibrocytes following their infiltration into the TAO orbit may determine their ultimate phenotype and thus their potential impact on tissue remodeling. A theoretical model of how Slit2 might regulate the participation of fibrocytes in the TAO orbit appears in Fig. 6. Our results may also have direct implications for other autoimmune diseases such as rheumatoid arthritis where fibrocytes have been detected in affected tissue (40). Examination of synovial fibroblasts in affected joint tissue for the generation of Slit2 might provide important insights into how fibrocytes are regulated in that disease process as well.

Supplementary Material

Refer to Web version on PubMed Central for supplementary material.

Acknowledgments

Grants: This work was supported in part by National Institutes of Health grants EY008976 and Autoimmune Center of Excellence grant 5UM1AI110498, Center for Vision grant EY007003 from the National Eye Institute, an unrestricted grant from Research to Prevent Blindness, and generous support from the Bell Charitable Foundation.

References

1. Bucala R, Spiegel LA, Chesney J, Hogan M, Cerami A. Circulating fibrocytes define a new leukocyte subpopulation that mediates tissue repair. Mol Med. 1994; 1:71–81. [PubMed: 8790603]
2. Chesney J, Metz C, Stavitsky AB, Bacher M, Bucala R. Regulated production of type I collagen and inflammatory cytokines by peripheral blood fibrocytes. J Immunol. 1998; 160:419–425. [PubMed: 9551999]
3. Abe R, Donnelly SC, Peng T, Bucala R, Metz CN. Peripheral blood fibrocytes: differentiation pathway and migration to wound sites. J Immunol. 2001; 166:7556–7562. [PubMed: 11390511]
4. Niedermeier M, Reich B, Rodriguez Gomez M, Denzel A, Schmidbauer K, Gobel N, Talke Y, Schweda F, Mack M. CD4+ T cells control the differentiation of Gr1+ monocytes into fibrocytes. Proc Natl Acad Sci U S A. 2009; 106:17892–17897. [PubMed: 19815530]
5. Chesney J, Bacher M, Bender A, Bucala R. The peripheral blood fibrocyte is a potent antigen-presenting cell capable of priming naive T cells in situ. Proc Natl Acad Sci U S A. 1997; 94:6307–6312. [PubMed: 9177213]

6. Crossno JT Jr, Majka SM, Grazia T, Gill RG, Klemm DJ. Rosiglitazone promotes development of a novel adipocyte population from bone marrow-derived circulating progenitor cells. J Clin Invest. 2006; 116:3220–3228. [PubMed: 17143331]

7. Fernando R, Vonberg A, Atkins SJ, Pietropaolo S, Pietropaolo M, Smith TJ. Human fibrocytes express multiple antigens associated with autoimmune endocrine diseases. J Clin Endocrinol Metab. 2014; 99:E796–803. [PubMed: 24517144]

8. Fernando R, Atkins S, Raychaudhuri N, Lu Y, Li B, Douglas RS, Smith TJ. Human fibrocytes coexpress thyroglobulin and thyrotropin receptor. Proc Natl Acad Sci U S A. 2012; 109:7427–7432. [PubMed: 22517745]

9. Smith TJ. TSH-receptor-expressing fibrocytes and thyroid-associated ophthalmopathy. Nat Rev Endocrinol. 2015; 11:171–181. [PubMed: 25560705]

10. Fernando R, Lu Y, Atkins SJ, Mester T, Branham K, Smith TJ. Expression of thyrotropin receptor, thyroglobulin, sodium-iodide symporter, and thyroperoxidase by fibrocytes depends on AIRE. J Clin Endocrinol Metab. 2014; 99:E1236–1244. [PubMed: 24708100]

11. Galligan CL, Keystone EC, Fish EN. Fibrocyte and T cell interactions promote disease pathogenesis in rheumatoid arthritis. J Autoimmun. 2016; 69:38–50. [PubMed: 26948996]

12. Kanasaki K, Taduri G, Koya D. Diabetic nephropathy: the role of inflammation in fibroblast activation and kidney fibrosis. Front Endocrinol (Lausanne). 2013; 4:7. [PubMed: 23390421]

13. Douglas RS, Afifiyan NF, Hwang CJ, Chong K, Haider U, Richards P, Gianoukakis AG, Smith TJ. Increased generation of fibrocytes in thyroid-associated ophthalmopathy. J Clin Endocrinol Metab. 2010; 95:430–438. [PubMed: 19897675]

14. Smith TJ. Rationale for therapeutic targeting insulin-like growth factor-1 receptor and bone marrow-derived fibrocytes in thyroid-associated ophthalmopathy. Expert Rev Ophthalmol. 2016; 11:77–79. [PubMed: 28603545]

15. Wang Y, Smith TJ. Current concepts in the molecular pathogenesis of thyroid-associated ophthalmopathy. Invest Ophthalmol Vis Sci. 2014; 55:1735–1748. [PubMed: 24651704]

16. Raychaudhuri N, Fernando R, Smith TJ. Thyrotropin regulates IL-6 expression in CD34+ fibrocytes: clear delineation of its cAMP-independent actions. PLoS One. 2013; 8:e75100. [PubMed: 24086448]

17. Li B, Smith TJ. Divergent expression of IL-1 receptor antagonists in CD34(+) fibrocytes and orbital fibroblasts in thyroid-associated ophthalmopathy: contribution of fibrocytes to orbital inflammation. J Clin Endocrinol Metab. 2013; 98:2783–2790. [PubMed: 23633206]

18. Brose K, Bland KS, Wang KH, Arnott D, Henzel W, Goodman CS, Tessier-Lavigne M, Kidd T. Slit proteins bind Robo receptors and have an evolutionarily conserved role in repulsive axon guidance. Cell. 1999; 96:795–806. [PubMed: 10102268]

19. Wang KH, Brose K, Arnott D, Kidd T, Goodman CS, Henzel W, Tessier-Lavigne M. Biochemical purification of a mammalian slit protein as a positive regulator of sensory axon elongation and branching. Cell. 1999; 96:771–784. [PubMed: 10102266]

20. Wu JY, Feng L, Park HT, Havlioglu N, Wen L, Tang H, Bacon KB, Jiang Z, Zhang X, Rao Y. The neuronal repellent Slit inhibits leukocyte chemotaxis induced by chemotactic factors. Nature. 2001; 410:948–952. [PubMed: 11309622]

21. Chen B, Blair DG, Plisov S, Vasiliev G, Perantoni AO, Chen Q, Athanasiou M, Wu JY, Oppenheim JJ, Yang D. Cutting edge: bone morphogenetic protein antagonists Drm/Gremlin and Dan interact with Slits and act as negative regulators of monocyte chemotaxis. J Immunol. 2004; 173:5914–5917. [PubMed: 15528323]

22. Glawe JD, Mijalis EM, Davis WC, Barlow SC, Gungor N, McVie R, Kevil CG. SDF-1-CXCR4 differentially regulates autoimmune diabetogenic T cell adhesion through ROBO1-SLIT2 interactions in mice. Diabetologia. 2013; 56:2222–2230. [PubMed: 23811810]

23. Peifer M, Fernandez-Cuesta L, Sos ML, George J, Seidel D, Kasper LH, Plenker D, Leenders F, Sun R, Zander T, Menon R, Koker M, Dahmen I, Muller C, Di Cerbo V, Schildhaus HU, Altmuller J, Baessmann I, Becker C, de Wilde B, Vandesompele J, Bohm D, Ansen S, Gabler F, Wilkening I, Heynck S, Heuckmann JM, Lu X, Carter SL, Cibulskis K, Banerji S, Getz G, Park KS, Rauh D, Grutter C, Fischer M, Pasqualucci L, Wright G, Wainer Z, Russell P, Petersen I, Chen Y, Stoelben E, Ludwig C, Schnabel P, Hoffmann H, Muley T, Brockmann M, Engel-Riedel W, Muscarella LA,

Fazio VM, Groen H, Timens W, Sietsma H, Thunnissen E, Smit E, Heideman DA, Snijders PJ, Cappuzzo F, Ligorio C, Damiani S, Field J, Solberg S, Brustugun OT, Lund-Iversen M, Sanger J, Clement JH, Soltermann A, Moch H, Weder W, Solomon B, Soria JC, Validire P, Besse B, Brambilla E, Brambilla C, Lantuejoul S, Lorimier P, Schneider PM, Hallek M, Pao W, Meyerson M, Sage J, Shendure J, Schneider R, Buttner R, Wolf J, Nurnberg P, Perner S, Heukamp LC, Brindle PK, Haas S, Thomas RK. Integrative genome analyses identify key somatic driver mutations of small-cell lung cancer. Nat Genet. 2012; 44:1104–1110. [PubMed: 22941188]

24. Dallol A, Da Silva NF, Viacava P, Minna JD, Bieche I, Maher ER, Latif F. SLIT2, a human homologue of the Drosophila Slit2 gene, has tumor suppressor activity and is frequently inactivated in lung and breast cancers. Cancer Res. 2002; 62:5874–5880. [PubMed: 12384551]
25. Kidd T, Bland KS, Goodman CS. Slit is the midline repellent for the robo receptor in Drosophila. Cell. 1999; 96:785–794. [PubMed: 10102267]
26. Pilling D, Zheng Z, Vakil V, Gomer RH. Fibroblasts secrete Slit2 to inhibit fibrocyte differentiation and fibrosis. Proc Natl Acad Sci U S A. 2014; 111:18291–18296. [PubMed: 25489114]
27. Sanders J, Jeffreys J, Depraetere H, Evans M, Richards T, Kiddie A, Brereton K, Premawardhana LD, Chirgadze DY, Nunez Miguel R, Blundell TL, Furmaniak J, Rees Smith B. Characteristics of a human monoclonal autoantibody to the thyrotropin receptor: sequence structure and function. Thyroid. 2004; 14:560–570. [PubMed: 15320966]
28. Smith TJ, Koumas L, Gagnon A, Bell A, Sempowski GD, Phipps RP, Sorisky A. Orbital fibroblast heterogeneity may determine the clinical presentation of thyroid-associated ophthalmopathy. J Clin Endocrinol Metab. 2002; 87:385–392. [PubMed: 11788681]
29. Pilling D, Fan T, Huang D, Kaul B, Gomer RH. Identification of markers that distinguish monocyte-derived fibrocytes from monocytes, macrophages, and fibroblasts. PLoS One. 2009; 4:e7475. [PubMed: 19834619]
30. Chedotal A. Slits and their receptors. Adv Exp Med Biol. 2007; 621:65–80. [PubMed: 18269211]
31. Ringstedt T, Braisted JE, Brose K, Kidd T, Goodman C, Tessier-Lavigne M, O'Leary DD. Slit inhibition of retinal axon growth and its role in retinal axon pathfinding and innervation patterns in the diencephalon. J Neurosci. 2000; 20:4983–4991. [PubMed: 10864956]
32. Xu HT, Yuan XB, Guan CB, Duan S, Wu CP, Feng L. Calcium signaling in chemorepellant Slit2-dependent regulation of neuronal migration. Proc Natl Acad Sci U S A. 2004; 101:4296–4301. [PubMed: 15020772]
33. Yiin JJ, Hu B, Jarzynka MJ, Feng H, Liu KW, Wu JY, Ma HI, Cheng SY. Slit2 inhibits glioma cell invasion in the brain by suppression of Cdc42 activity. Neuro Oncol. 2009; 11:779–789. [PubMed: 20008733]
34. Gu JJ, Gao GZ, Zhang SM. miR-218 inhibits the migration and invasion of glioma U87 cells through the Slit2-Robo1 pathway. Oncol Lett. 2015; 9:1561–1566. [PubMed: 25789001]
35. Bekes I, Haunerdinger V, Sauter R, Holzheu I, Janni W, Wockel A, Wulff C. Slit2/Robo4 Signaling: Potential Role of a VEGF-Antagonist Pathway to Regulate Luteal Permeability. Geburtshilfe Frauenheilkd. 2017; 77:73–80. [PubMed: 28190892]
36. Mukovozov I, Huang YW, Zhang Q, Liu GY, Siu A, Sokolskyy Y, Patel S, Hyduk SJ, Kutryk MJ, Cybulsky MI, Robinson LA. The Neurorepellent Slit2 Inhibits Postadhesion Stabilization of Monocytes Tethered to Vascular Endothelial Cells. J Immunol. 2015; 195:3334–3344. [PubMed: 26297762]
37. Guan H, Zu G, Xie Y, Tang H, Johnson M, Xu X, Kevil C, Xiong WC, Elmets C, Rao Y, Wu JY, Xu H. Neuronal repellent Slit2 inhibits dendritic cell migration and the development of immune responses. J Immunol. 2003; 171:6519–6526. [PubMed: 14662852]
38. Smith TJ, Hegedus L. Graves' Disease. N Engl J Med. 2016; 375:1552–1565. [PubMed: 27797318]
39. Gillespie EF, Papageorgiou KI, Fernando R, Raychaudhuri N, Cockerham KP, Charara LK, Goncalves AC, Zhao SX, Ginter A, Lu Y, Smith TJ, Douglas RS. Increased expression of TSH receptor by fibrocytes in thyroid-associated ophthalmopathy leads to chemokine production. J Clin Endocrinol Metab. 2012; 97:E740–746. [PubMed: 22399514]
40. Galligan CL, Siminovitch KA, Keystone EC, Bykerk V, Perez OD, Fish EN. Fibrocyte activation in rheumatoid arthritis. Rheumatology (Oxford). 2010; 49:640–651. [PubMed: 19858121]

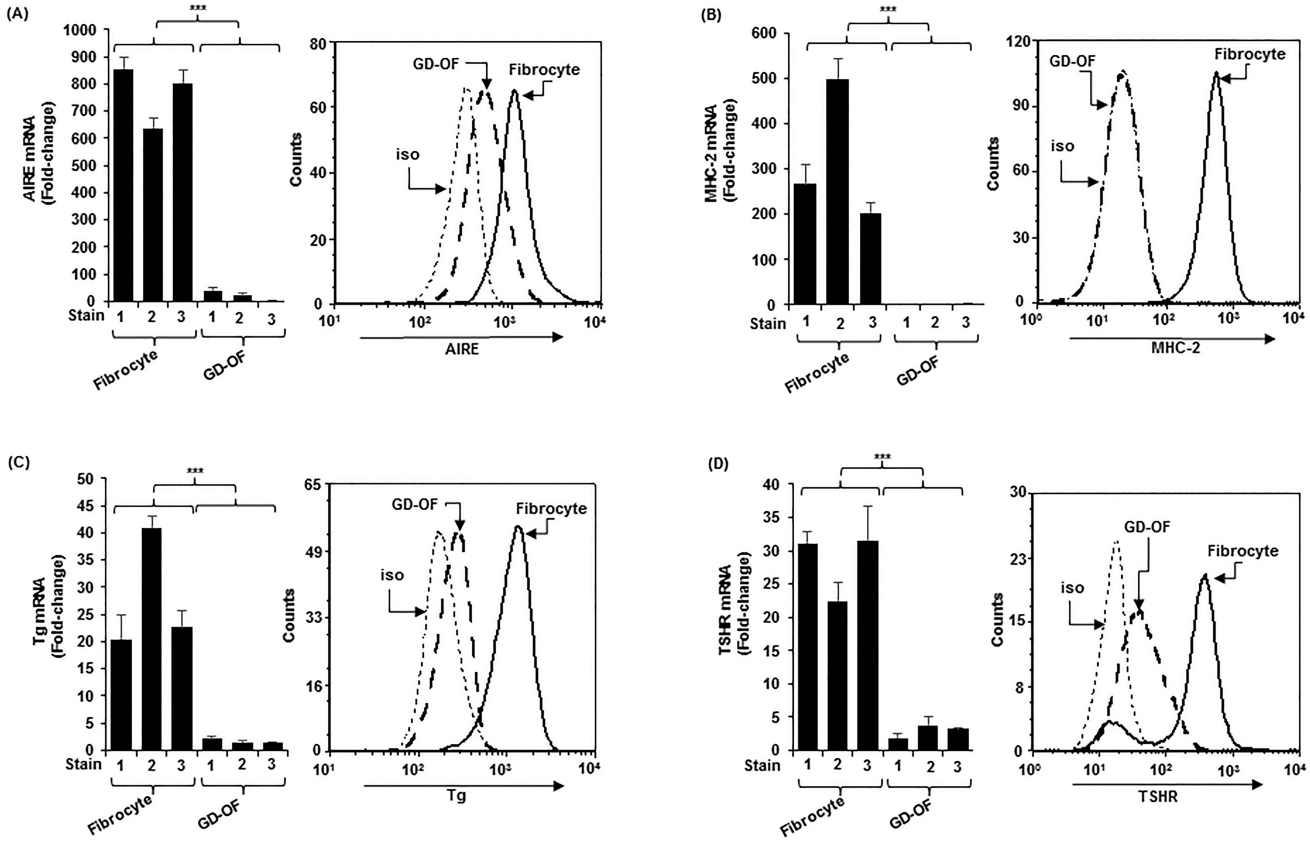

Figure 1.

Higher levels of (A) autoimmune regulator protein (AIRE), (B) MHC Class II (MHC-2) (C) thyroglobulin (Tg), (D) thyrotropin receptor (TSHR) in fibrocytes than orbital fibroblasts from patients with Graves' disease (GD-OF). Confluent cell layers were harvested and (left panels) RNA isolated, reverse-transcribed, and subjected to real-time PCR and (right panels) stained with the labeled antibodies for flow cytometry as described in the Methods section. mRNA data were normalized to their respective GAPDH levels and are expressed as the mean ± SD of triplicate determinations. MFI data: AIRE, fibrocytes, 813.35 ± 30.18 vs GD-OF, 223.35 ± 31.2 (4-fold); MHC-2, fibrocytes, 490.56 ± 13.35 vs GD-OF, 18.73 ± 17.82 (11,797-fold); Tg, fibrocytes, 965.97 ± 21.85 vs GD-OF, 14.35 ± 15.84 67-fold); TSHR, fibrocytes, 193.58 ± 24.2 vs GD-OF, 26.92 ± 18.82 (7-fold). Data from flow analysis denote fluorescence intensity compared with isotype controls. *** $P<0.001$. A total of three experiments were performed.

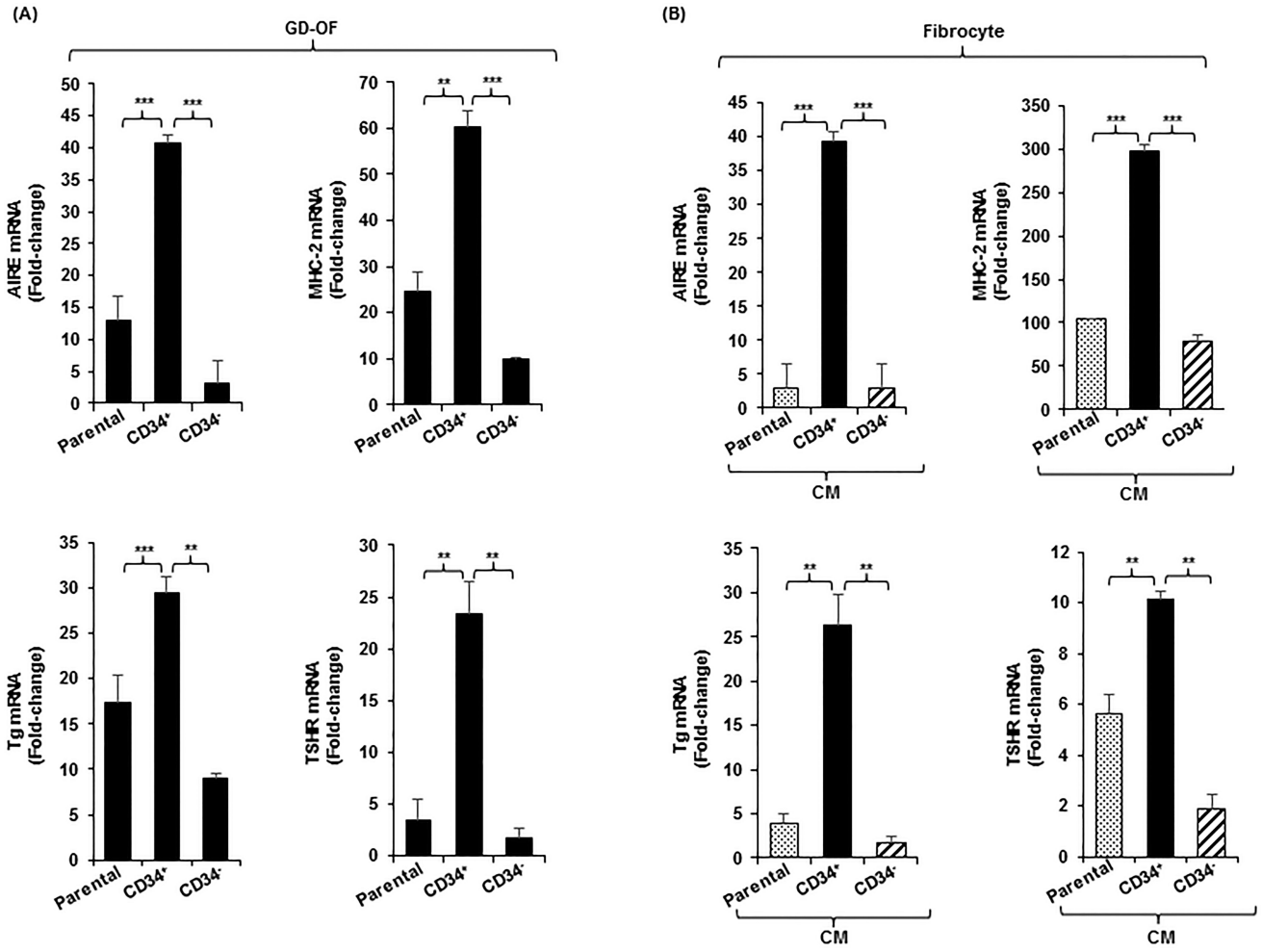

Figure 2.

(A) Expression pattern of AIRE, MHC-2, Tg, and TSHR in parental (mixed) GD-OF and pure $CD34^+$ OF and $CD34^-$ OF subsets. Parental GD-OF strains were subjected to sham cytometric sorting or sorted into $CD34^+$ OF and $CD34^-$ OF subsets and cultured for 3 d. (B) Conditioned media were generated by incubating GD-OF ▨, $CD34^+$ OF ■, and $CD34^-$ OF ▨ in DMEM for 48 h. These media were then used to cover fibrocytes for 3 d. Monolayers were harvested, RNA extracted, reverse-transcribed and subjected to real-time PCR. Data are expressed as the mean ± SD of 3 independent replicates. Values were normalized to their respective GAPDH levels and are expressed as mean ± SD of triplicate determinations. *** $p<0.001$; ** $p<0.01$. Experiments were performed three times.

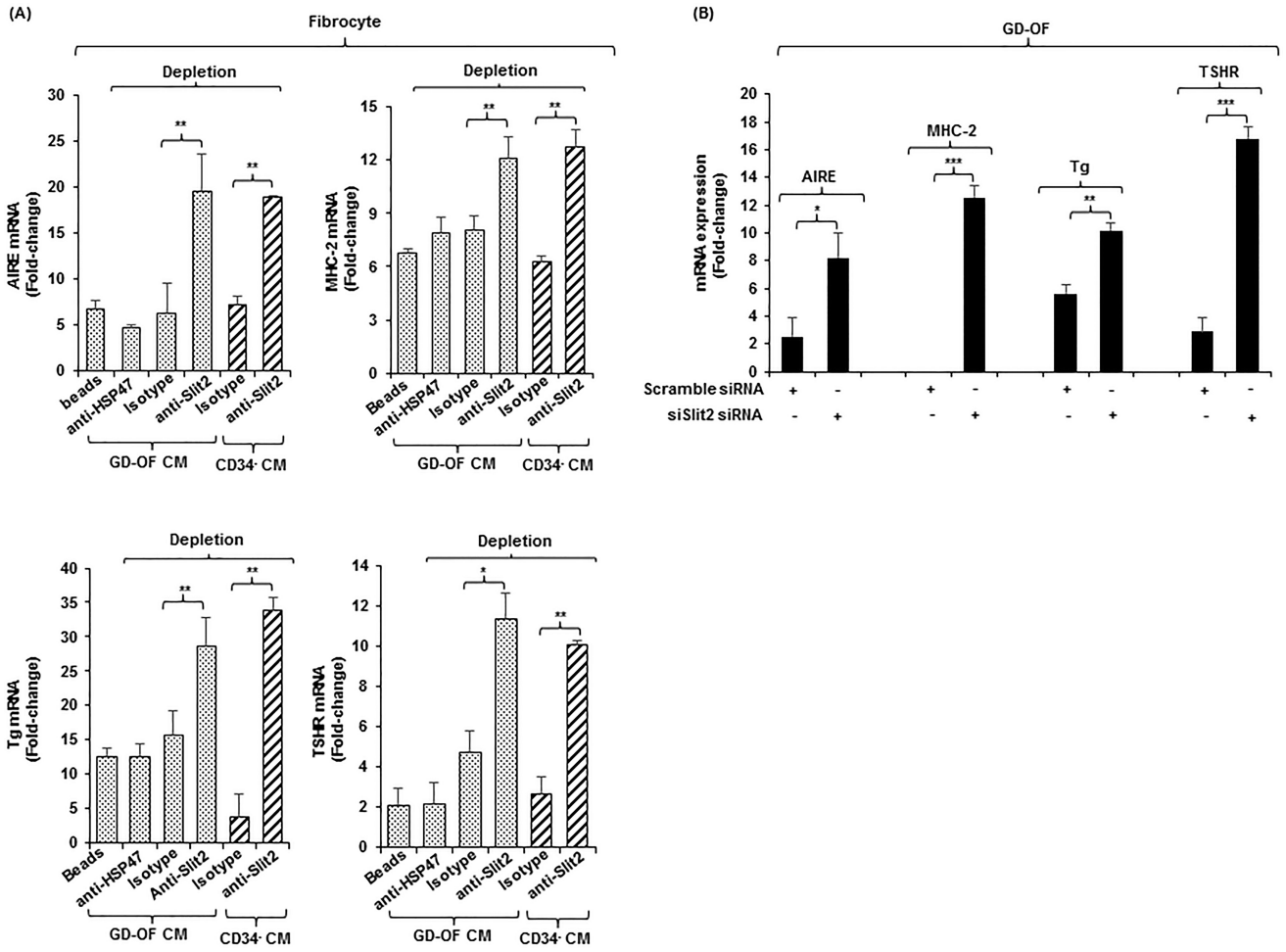

Figure 3.

(A) Depleting medium conditioned by GD-OF of Slit2 restores fibrocyte gene expression. (A) Conditioned media (CM) from GD-OF ▒and CD34⁻ OF ▨were incubated with uncoated beads or beads coated with anti-Slit2 (100 μg), anti-HSP47 (100 μg), or isotype IgG (100 μg) as described in Methods. Fibrocyte monolayers were incubated with these media for 5 d. (B) Knocking down Slit2 with specific siRNA enhances gene expression in GD-OF. GD-OF were transfected with either scrambled (control) siRNA (3μg) or Slit2-specific siRNA (3μg) and incubated 3 d. RNA was extracted, reversed transcribed, and cDNAs subjected to real-time PCR for the targets indicated. Values were normalized to their respective GAPDH levels and expressed as mean ± SD of triplicate determinations. *** $p<0.001$, ** $p<0.01$; * $p<0.05$. Experiments were performed three times.

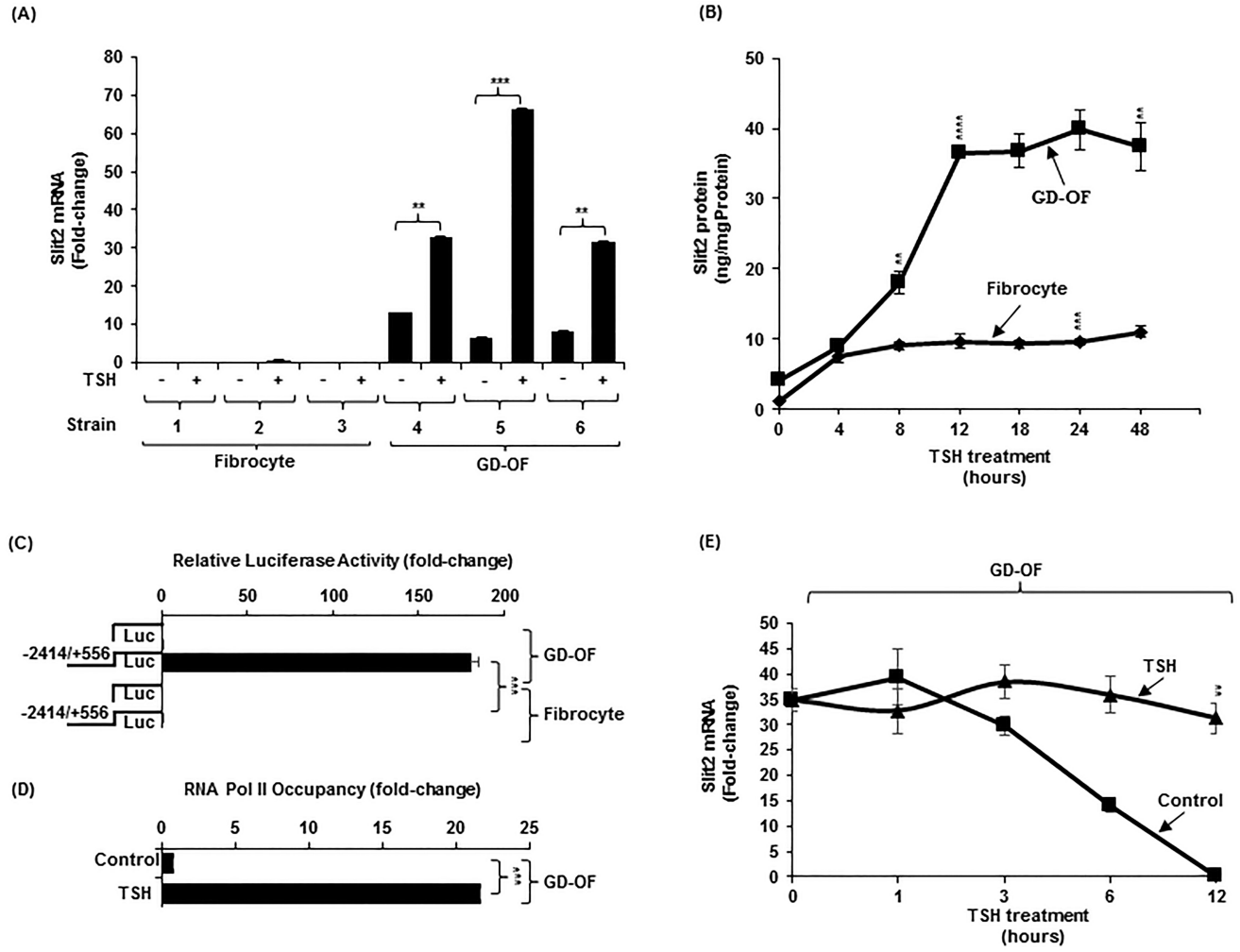

Figure 4.

Slit2 is preferentially expressed in GD-OF compared to fibrocytes. It is a TSH-inducible protein as a consequence of increased gene transcription and mRNA stability. (A). Three strains of confluent fibrocytes and GD-OF remained untreated or were treated with bTSH (5mIU/ml) for 6 h, RNA extracted, reversed transcribed, and cDNA subjected to real-time PCR for Slit2. (B) Fibrocytes and GD-OF were treated with bTSH (5mIU/ml) for the graded intervals indicated along the abscissa. Medium was collected and subjected to a specific Slit2 ELISA as described in Methods. (C) A 2970 bp fragment of the human Slit2 gene promoter was cloned as described in Methods and transfected into fibrocytes and GD-OF. Cell layers were assayed for luciferase activity. (D) Confluent GD-OF were untreated or treated with bTSH for 2 h and subjected to a ChiP transcription assay as detailed in Methods. (E) GD-OF were pre-treated with bTSH for 2 h. All cultures were treated at time "0" with DRB (20 μg/mL) without or in the continued presence of bTSH for the intervals indicated along the abscissa. RNA was extracted, reverse transcribed, and subjected to real-time quantitative PCR for Slit2. Values were normalized to their respective GAPDH levels. Slit2 ELISA, luciferase assay, and ChiP results were normalized to the respective protein

levels. Data were expressed as the mean ± SD of triplicate determinations. *** $p<0.001$,** $p<0.01$. Experiments were performed three times.

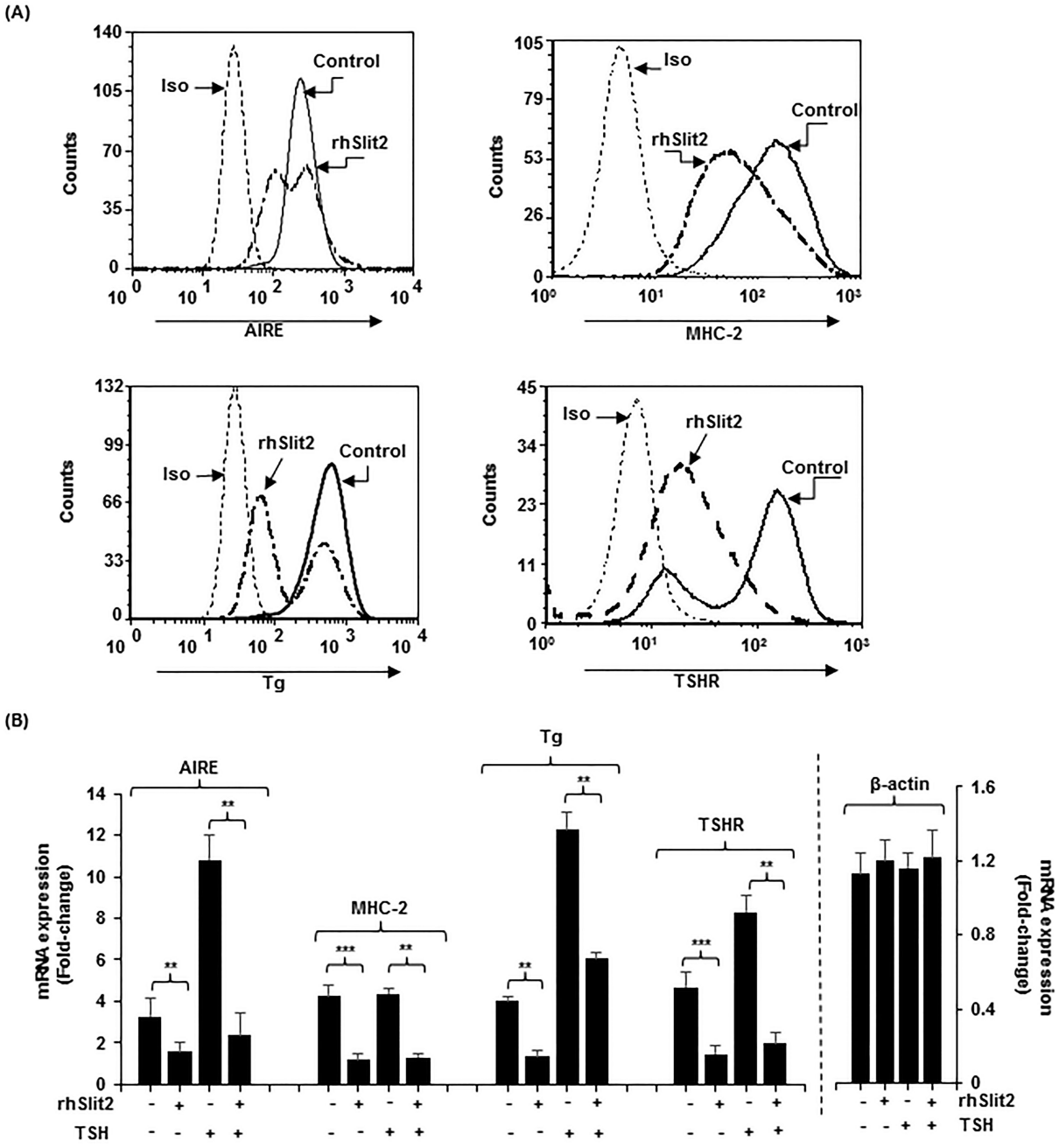

Figure 5.

rhSlit2 attenuates expression of AIRE, MHC-2, Tg and TSHR in fibrocytes. (A) Cultured PBMCs were treated with rhSlit2 (50ng/mL) for 7–9 d, fibrocyte monolayers were harvested, stained with the antibodies indicated and subjected to flow cytometric analysis. (B) Fibrocytes were untreated or treated with rhSlit2 and then some were treated with bTSH for 6 h, monolayers harvested, RNA was extracted, reverse-transcribed, and subjected to real-time PCR for the targets indicated. Values were normalized to their respective GAPDH levels and β-actin levels and are expressed as the mean ± SD of triplicate determinations. ** $p<0.01$. Experiments were performed three times.

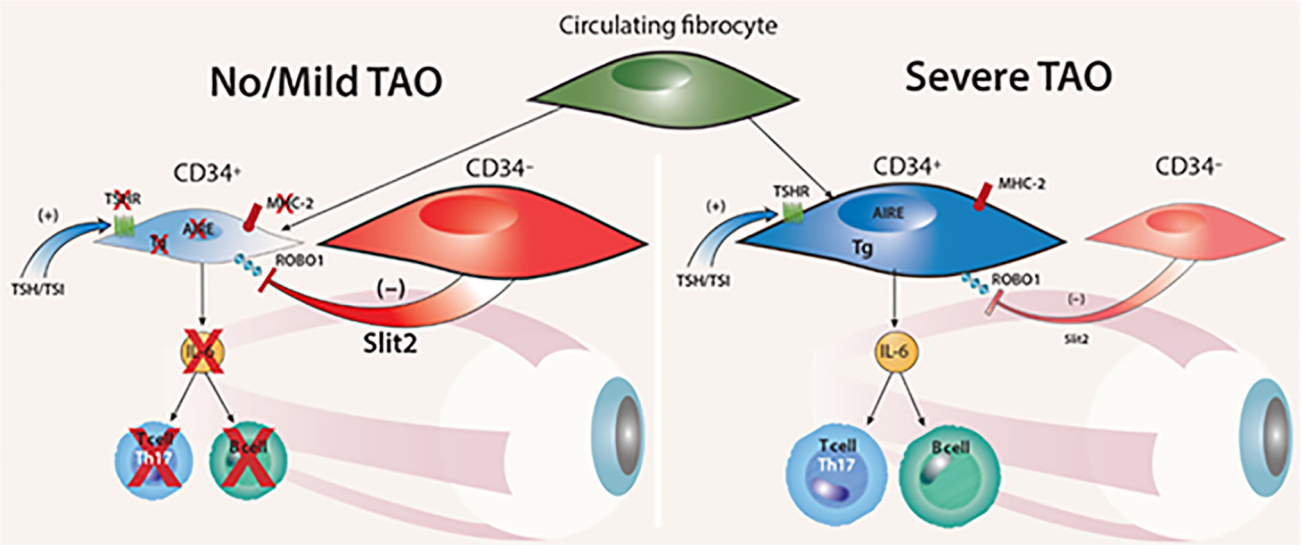

Figure 6.

Theoretical model for the modulatory role of Slit2 on intra-orbital pathogenesis of TAO. When $CD34^{-}$ OF-derived Slit2 predominates, the inflammatory phenotype of $CD34^{+}$ OF is down regulated and the patient with GD either fails to manifest TAO or the disease is mild (Left panel). When $CD34^{+}$ OF dominates the fibroblast population and the impact of Slit2 is inadequate, TAO is severe (Right panel).